*Thermochimica Acta*, 181 (1991) 45–56
Elsevier Science Publishers B.V., Amsterdam

# KINETICS AND MECHANISM OF DEHYDRATION OF NATROLITE AND ITS POTASSIUM EXCHANGED FORM

R. OTSUKA, A. YAMAZAKI and K. KATO

*Department of Mineral Resources Engineering, School of Science and Engineering, Waseda University, 4-1, Okubo 3 Chome, Shinjuku-ku, Tokyo 169 (Japan)*

(Received 24 August 1990)

## ABSTRACT

A kinetic analysis was done of the dehydration in natrolite and its corresponding potassium exchanged form. Kinetic evaluation of the thermogravimetric data based on Ozawa's methods yielded the following results: the activation energy is 126.83 kJ $mol^{-1}$ for natrolite and 74.01 kJ $mol^{-1}$ for the potassium form, the frequency factor is $1.92 \times 10^9$ $s^{-1}$ for natrolite and $3.31 \times 10^7$ $s^{-1}$ for the potassium form, and the dehydration follows zero-order kinetics in natrolite and first-order kinetics in the potassium form. Considering the crystal structures of the hydrated and dehydrated phases of natrolite and its potassium form, together with the results of the kinetic analysis, it is suggested that the dehydration in natrolite proceeds at a constant rate in one direction parallel to the *c* axis, while in the potassium exchange form the dehydration is instantly completed in each particle and then proceeds particle by particle.

## INTRODUCTION

Natrolite is a fibrous aluminosilicate belonging to the fibrous zeolite group, the ideal chemical formula of which is $Na_{16}Si_{24}Al_{16}O_{80} \cdot 16H_2O$. The thermal behaviour of this mineral has been studied by many workers [1–6]. According to them, natrolite dehydrates abruptly in a single step over the temperature range 250–400 °C and changes to $\alpha$-metanatrolite. Furthermore, several workers have reported the structure change of this mineral due to dehydration [7–11]. However, no kinetic study of the dehydration of natrolite has been carried out, with the exception of the work by Tanabe [12]. More recently, the present authors have obtained the potassium exchanged form of natrolite, the occurrence of which in nature has not yet been reported, and investigated its structure and thermal properties [13–15]. In the present study, a kinetic analysis of the dehydration of natrolite and its potassium exchanged form was carried out and the dehydration mechanisms of the processes were considered in comparison with each other.

## EXPERIMENTAL

Natrolite (Yanai, Shinjo City, Aichi Pref., Japan; National Science Museum NSM M-21497) was carefully purified by hand-picking under binoculars, and then sieved to under 200 mesh.

The potassium exchanged form of natrolite (K-form) was obtained as follows: 200 mg of natrolite (under 200 mesh) was treated with 100 ml of 1 N KCl solution (pH 8–9) in a 300-ml flask at 60 °C for 60 days. The products were dried at 60 °C, and then kept in a desiccator for more than 3 days, during which time the relative humidity was maintained at about 55% with saturated $Mg(NO_3)_2$ solution, until they were subjected to subsequent measurements.

The chemical composition of the samples was determined with an electron-probe microanalyser (JEOL, Type JXA733), giving the results listed in Table 1. In the K-form used in this study, the degree of potassium exchange was 98.6%. Here, the degree is expressed as $[K_2O/(Na_2O + K_2O + MgO + CaO)] \times 100\%$ (oxides in mole). Thermogravimetric/differential thermal analysis (TG-DTA) curves were recorded on a Rigaku Thermoflex TG-DTA unit in flowing nitrogen (100 ml $min^{-1}$). The sample weight used was 15.0 mg. The heating rate was programmed as 20, 10, 5 or 2.5 K $min^{-1}$.

TABLE 1

Chemical composition and number of cations of natrolite and its K-form on the basis of 80(O)

| | wt% | | Number of cations | | |
|---|---|---|---|---|---|
| | Natrolite [a] | K-form [b] | | Natrolite [a] | K-form [b] |
| $SiO_2$ | 47.08 | 43.0 | Si | 23.97 | 24.2 |
| $Al_2O_3$ | 26.56 | 23.7 | Al | 15.94 | 15.7 |
| FeO [c] | 0.00 | 0.0 | Fe [c] | 0.00 | 0.0 |
| CaO | 0.17 | 0.3 | Ca | 0.01 | 0.2 |
| MgO | 0.00 | 0.0 | Mg | 0.00 | 0.0 |
| SrO | 0.00 | 0.0 | Sr | 0.00 | 0.0 |
| BaO | 0.00 | 0.0 | Ba | 0.00 | 0.0 |
| $Na_2O$ | 16.47 | 0.2 | Na | 16.26 | 0.2 |
| $K_2O$ | 0.00 | 22.0 | K | 0.00 | 15.8 |
| $H_2O$ | 9.72 | 10.8 | | | |
| Total | 100.00 | 100.00 | $E$ [d] (%) | −2.1 | −1.7 |
| | | | $K$ [e] (%) | 0.0 | 98.6 |

[a] Single crystals were analysed by means of the wavelength dispersion method. [b] Powder specimens were analysed by means of the energy dispersion method. [c] Total Fe as FeO. [d] $E$ (balance error) = $\{(Al + Fe^{3+}) - [Na + K + 2(Ca + Mg)]\}/[Na + K + 2(Ca + Mg)] \times 100\%$. [e] $K = [K_2O/(Na_2O + K_2O + MgO + CaO + SrO + BaO)] \times 100\%$.

## RESULTS AND DISCUSSION

The DTA curves of natrolite and its K-form are shown in Fig. 1. Figure 1(A) shows the typical DTA patterns of natrolite. It is characterized by a large and sharp endotherm at 342° C due to a one-step dehydration and a very small endotherm at 517° C corresponding to the phase transition from $\alpha$- to $\beta$-*meta*-natrolite. The DTA curve of the K-form (Fig. 1(B)) has a remarkable single endotherm at 151° C due to dehydration. The thermal behaviour of the K-form has been reported previously by the present authors [13].

### *Kinetic analysis*

The kinetic analysis was carried out using the methods of Ozawa [16,17]. The thermal decomposition of a solid is generally expressed as

$$A(s) = B(s) + C(g) \quad (1)$$

where A is the reactant, B and C are the products, and (s) and (g) designate solid and gaseous phases, respectively.

The reaction rate under isothermal conditions can be described as

$$d\alpha/dt = Z \cdot \exp(-E/RT) \cdot f(\alpha) \quad (2)$$

where $\alpha$, $t$, $Z$, $E$, $R$ and $T$ are the fraction conversion, the time, the pre-exponential factor, the activation energy, the gas constant and the absolute temperature, respectively; $f(\alpha)$ is a function depending on the reaction mechanism.

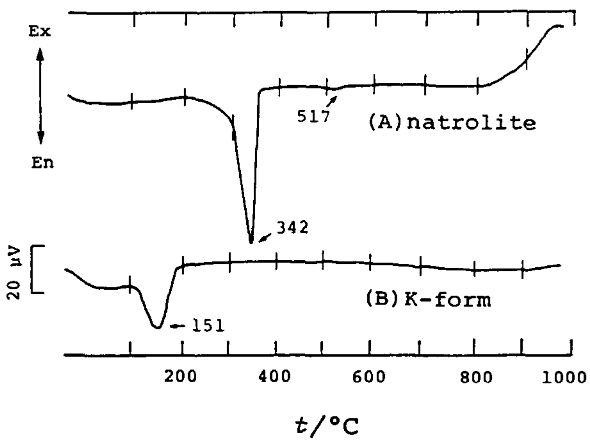

Fig. 1. DTA curves of (A) natrolite and (B) its K-form.

If the temperature rise is linear, $\nu = \mathrm{d}T/\mathrm{d}t$, then

$$\mathrm{d}\alpha/\mathrm{d}t = Z/\nu \exp(-E/RT) \cdot f(\alpha) \tag{3}$$

where $\nu$ is the heating rate.

From eqn. (3),

$$g(\alpha) = [\mathrm{d}\alpha/f(\alpha)] = ZE/\nu R \cdot p(x) \tag{4}$$

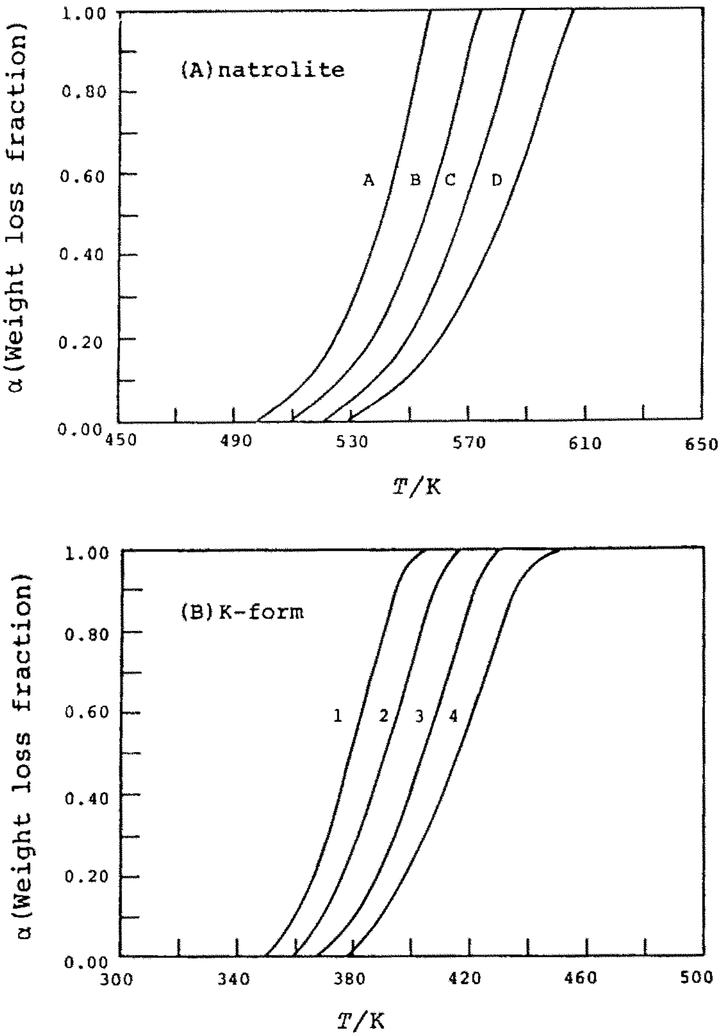

Fig. 2. (A) Plots of $\alpha$ (weight loss fraction) vs. $T$ for the dehydration of natrolite. Heating rate (K $\text{min}^{-1}$): A, 2.5, B, 5, C, 10, D, 20. (B) Plots of $\alpha$ (weight loss fraction) vs. $T$ for the dehydration of the K-form. Heating rate (K $\text{min}^{-1}$): (1) 2.5, (2) 5, (3) 10, (4) 20.

where $p(x)$ is the function introduced by Doyle [18] and $x = E/RT$. If $x$ is larger than 20, $p(x)$ can be expressed as

$$\log p(x) = -2.315 - 0.4567x \tag{5}$$

Taking the logarithm of eqn. (4), and substituting eqn. (5) into the right-hand side of eqn. (4) gives

$$\log g(\alpha) = (\log ZE/\nu R - 2.315) - 0.4567E/RT \tag{6}$$

or

$$\log \nu = -2.315 + \log[ZE/Rg(\alpha)] - 0.4567E/RT \tag{7}$$

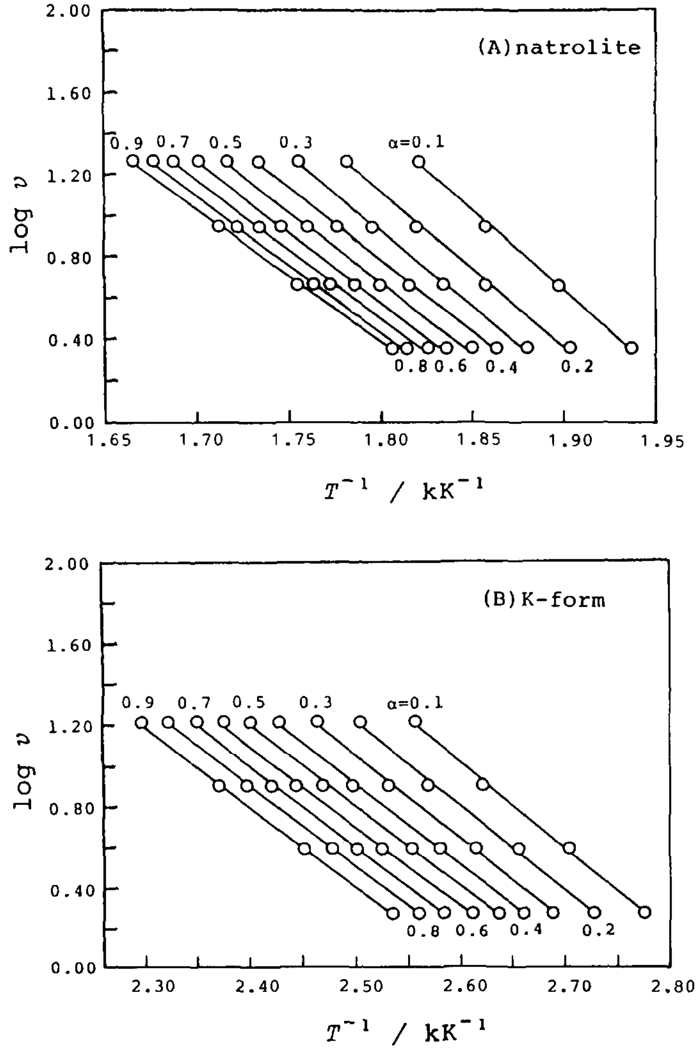

Fig. 3. Plots of log $\nu$ vs. $1/T$ for different $\alpha$ of the dehydration of (A) natrolite and (B) its K-form.

TABLE 2

Kinetic analysis of the dehydration of natrolite

| $\alpha$ | $E$ (kJ mol$^{-1}$) | $1/T_e$ [a] (kK$^{-1}$) | $\theta$ ($\times 10^{-3}$ $\mu$s) |
|---|---|---|---|
| 0.05 | 144.91 | 2.008 | 0.045 |
| 0.10 | 141.48 | 1.984 | 0.066 |
| 0.15 | 139.15 | 1.964 | 0.091 |
| 0.20 | 135.83 | 1.951 | 0.111 |
| 0.25 | 134.64 | 1.939 | 0.135 |
| 0.30 | 133.91 | 1.928 | 0.162 |
| 0.35 | 129.12 | 1.923 | 0.173 |
| 0.40 | 128.71 | 1.913 | 0.206 |
| 0.45 | 127.97 | 1.906 | 0.230 |
| 0.50 | 125.35 | 1.901 | 0.249 |
| 0.55 | 124.04 | 1.895 | 0.274 |
| 0.60 | 124.05 | 1.888 | 0.307 |
| 0.65 | 122.71 | 1.882 | 0.338 |
| 0.70 | 121.11 | 1.878 | 0.360 |
| 0.75 | 121.02 | 1.873 | 0.391 |
| 0.80 | 120.27 | 1.868 | 0.423 |
| 0.85 | 119.10 | 1.864 | 0.451 |
| 0.90 | 117.71 | 1.861 | 0.474 |
| 0.95 | 115.20 | 1.858 | 0.497 |

[a] $T_e$ values were obtained by extrapolating plots of log $\nu$ vs. $1/T$ for each $\alpha$ to log $\nu = 0$ ($\nu = 1$ K min$^{-1}$) in Fig. 3(A).

Equation (7) indicates that log $\nu$ vs. $1/T$ plots for a given value of $\alpha$ give a straight line, the slope of which gives the activation energy $E$ [16]. Figure 2 shows plots of $\alpha$ vs. $T$ for natrolite and its K-form, which were derived from TG curves under different heating rates. Using these data, log $\nu$ was plotted vs. $1/T$ for 19 values of $\alpha$, ranging from 0.05 to 0.95, at 0.05 intervals (Fig. 3). The parallel straight lines were obtained over almost the entire range of $\alpha$, especially in the $\alpha$ range 0.2–0.8 for both natrolite and its K-form. The values of $E$ for each value of $\alpha$ are listed in Tables 2 (natrolite) and 3 (K-form). The average $E$ values are $126.83 \pm 5.17$ kJ mol$^{-1}$ for natrolite ($\alpha = 0.2$–$0.8$) and $74.01 \pm 1.46$ kJ mol$^{-1}$ for the K-form ($\alpha = 0.2$–$0.8$).

Ozawa [16,17] introduced the reduced time, $\theta$, which is expressed as

$$\theta = E/\nu R \cdot p(x) \tag{8}$$

Taking the logarithm of eqn. (8) and substituting eqn. (5) into the right-hand side of eqn. (8) gives

$$\log \theta = \log(E/\nu R) - (2.315 + 0.4567E/RT) \tag{9}$$

If $T = T_e$ when $\nu = 1$ K min$^{-1}$, $T_e$ can be determined by extrapolating log$\nu$ vs. $1/T$ plots for each $\alpha$ to log $\nu = 0$. The values of $\theta$ can be

TABLE 3

Kinetic analysis of the dehydration of the K-form of natrolite

| $\alpha$ | $E$ (kJ $mol^{-1}$) | $1/T_e$ [a] ($kK^{-1}$) | $\theta$ ($\mu$s) |
|---|---|---|---|
| 0.05 | 81.65 | 2.865 | 0.006 |
| 0.10 | 78.22 | 2.839 | 0.007 |
| 0.15 | 77.95 | 2.813 | 0.010 |
| 0.20 | 76.89 | 2.792 | 0.012 |
| 0.25 | 76.51 | 2.772 | 0.014 |
| 0.30 | 76.53 | 2.753 | 0.017 |
| 0.35 | 75.16 | 2.740 | 0.019 |
| 0.40 | 74.21 | 2.726 | 0.021 |
| 0.45 | 73.25 | 2.715 | 0.024 |
| 0.50 | 72.62 | 2.704 | 0.026 |
| 0.55 | 73.05 | 2.690 | 0.032 |
| 0.60 | 73.17 | 2.676 | 0.034 |
| 0.65 | 72.46 | 2.665 | 0.038 |
| 0.70 | 73.01 | 2.651 | 0.043 |
| 0.75 | 72.71 | 2.640 | 0.048 |
| 0.80 | 72.52 | 2.628 | 0.054 |
| 0.85 | 72.02 | 2.616 | 0.060 |
| 0.90 | 72.36 | 2.602 | 0.068 |
| 0.95 | 70.94 | 2.586 | 0.080 |

[a] $T_e$ values were obtained by extrapolating plots of $\log \nu$ vs. $1/T$ for each $\alpha$ to $\log \nu = 0$ ($\nu = 1$ K $min^{-1}$) in Fig. 3(B).

determined from the average values of $E$ and $1/T$ for each $\alpha$. These data are also listed in Tables 2 (natrolite) and 3 (K-form).

Substituting $\theta$ into eqn. (4), gives

$$g(\alpha) = Z \cdot \theta \tag{10}$$

Hence, if $g(\alpha)$ expresses the correct mechanism, a plot of $g(\alpha)$ vs. $\theta$ will give a straight line, the slope of which is equal to $Z$, the pre-exponential factor. Figure 4 illustrates plots of $g(\alpha)$ vs. $\theta$ for natrolite and its K-form at various $g(\alpha)$ in commonly used kinetic equations [19]. The plots show the best linearity when $g(\alpha) = \alpha = kt$ (R1) (zero-order reaction) in the range of $\alpha = 0.2$ to 0.8 for natrolite and $g(\alpha) = -\ln(1-\alpha) = kt$ (F1) (first-order reaction) in the $\alpha$ range 0.2–0.8 for the K-form. From the slope of the straight-line plot, $Z$ values were estimated as $1.92 \times 10^9$ $s^{-1}$ for natrolite and $3.31 \times 10^7$ $s^{-1}$ for its K-form. The results of the kinetic analysis are summarized in Table 4.

Figure 5 shows the chain structure of natrolite parallel to the $c$ axis. The structure is made up of $SiO_4$ and $AlO_4$ tetrahedra. The structures of natrolite and dehydrated natrolite at 350 °C projected along the $c$ axis are illustrated in Fig. 6(A). The latter structure was determined by Alberti and Vezzalini [10]. In natrolite, Na cations and water molecules are in the channel parallel

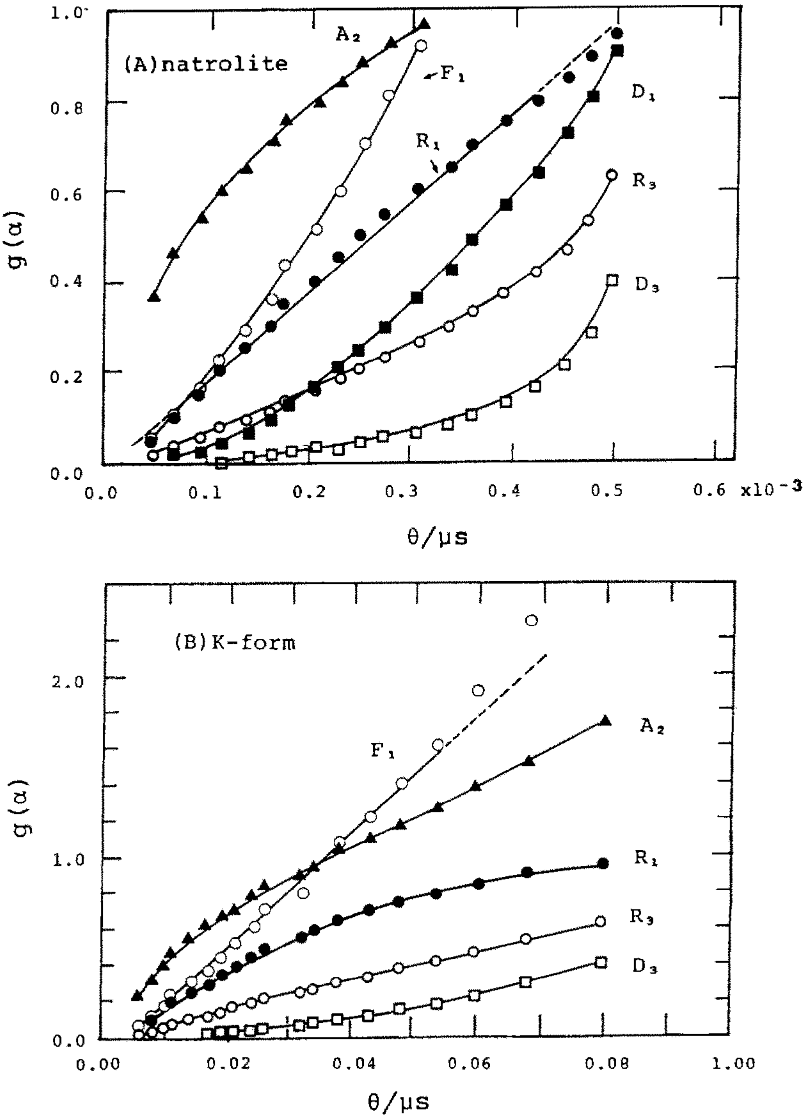

Fig. 4. Plots of $g(\alpha)$ vs. $\theta$ for various kinetic equations of the dehydration of (A) natrolite and (B) its K-form.

TABLE 4

Kinetic parameters and reaction mechanism of natrolite and its K-form

| | $E$ (kJ $\text{mol}^{-1}$) | $Z$ ($\text{s}^{-1}$) | Reaction mechanism (function, equation) |
|---|---|---|---|
| Natrolite | 126.83 | $1.92 \times 10^9$ | $R_1$, $g(\alpha) = \alpha = kt$ |
| K-form | 74.01 | $3.31 \times 10^7$ | $F_1$, $g_\alpha = -\ln(1-\alpha) = kt$ |

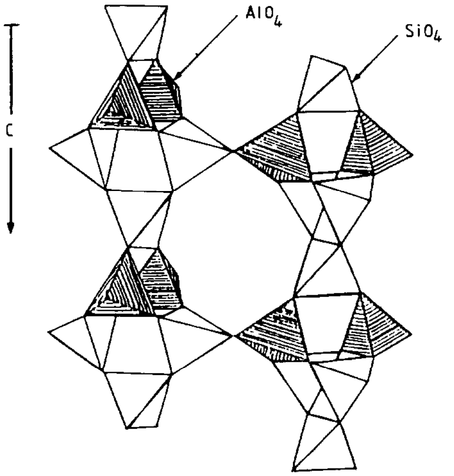

Fig. 5. Chain structures of (Si, Al) tetrahedra in natrolite [7].

to *c*. The water molecules are near to the port between channels [11]. According to Alberti and Vezzalini [10], the most striking change in the framework of dehydrated natrolite is the rotation of the tetrahedral chain around its axis parallel to *c*. As a result, *a* and *b* contract by 11.2 and 8.5%, respectively (Table 5). Sodium atoms migrate to sites near those occupied by water molecules in natrolite. Furthermore, it is generally accepted that the dehydration of natrolite proceeds through the channels parallel to *c*. However, Meier [7] considered that the dehydration occurs through the intersecting channels between neighbouring chains, and thus perpendicular to *c*, since the channels parallel to *c* are much narrower. Later, Peacor [9], by the means of direct observation of the natrolite crystal, confirmed that dehydration must occur with diffusion of $H_2O$ through the channels parallel to *c*.

The results of the kinetic analysis indicate that the dehydration of natrolite follows zero-order kinetics. In the zero-order reaction, the reaction

TABLE 5

Lattice parameters of hydrated and dehydrated phases of natrolite and its K-form

| | | Bond length (Å) | |
|---|---|---|---|
| | | Hydrated phase | Dehydrated phase |
| Natrolite | *a* | 18.304 (2) | 16.254 (11) [a] |
| | *b* | 18.645 (4) | 17.066 (11) [a] |
| | *c* | 6.592 (2) | 6.436 (4) [a] |
| K-form | *a* | 19.278 (5) | 17.133 (18) [b] |
| | *b* | 19.737 (5) | 18.246 (20) [b] |
| | *c* | 6.484 (2) | 6.517 (9) [b] |

[a] At 350 °C. [b] At 300 °C.

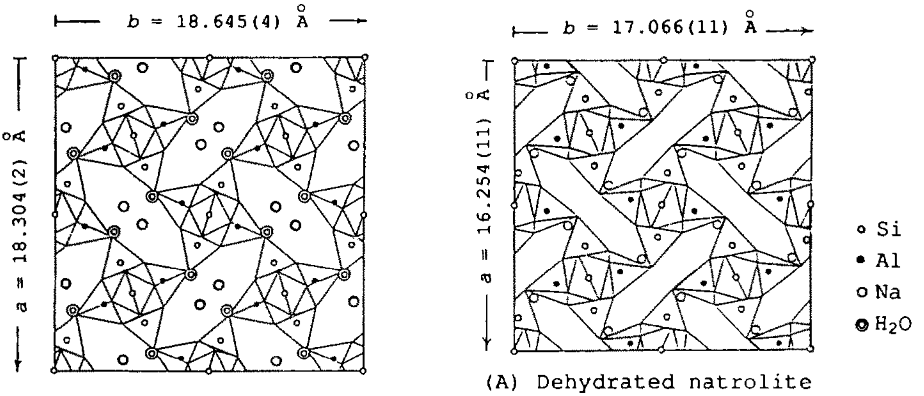

(A) natrolite

(A) Dehydrated natrolite at 350 °C (after Alberti and Vezzalini (1983))

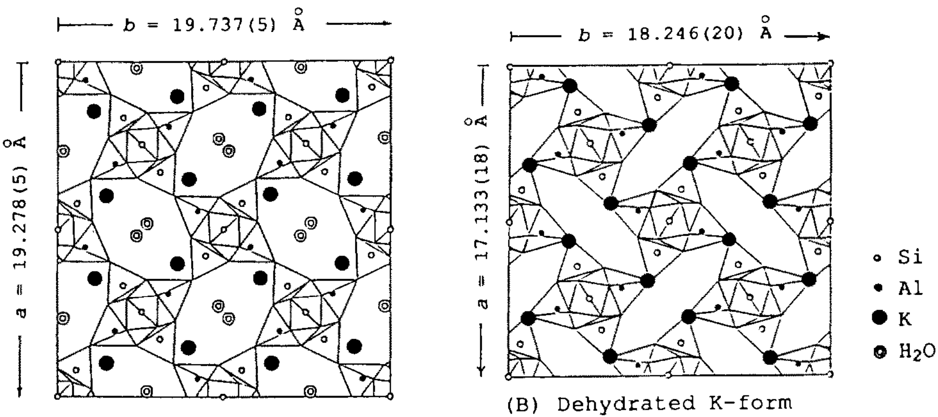

(B) K-form

(B) Dehydrated K-form at 300 °C

Fig. 6. (A) Crystal structures of natrolite and dehydrated natrolite at 350 °C projected along *c* [10]. (B) Crystal structures of the K-form and the dehydrated K-form at 300 °C projected along *c* [14].

proceeds at a constant rate for all, or the greater part of, the process. Hence, as the reaction model of natrolite, it is considered that the interface separating hydrated and dehydrated phases advances at a constant rate in a single direction parallel to *c*, with the propagation of the rotation of the tetrahedral chain.

Figure 6(B) shows the structures of the K-form and dehydrated K-form at 300 °C projected along *c*. The former structure was determined using the Rietveld method [14], while the latter was derived from the comparison of the observed X-ray diffraction patterns with the simulated ones. In the K-form, the K ions are coordinated with each oxygen atom of eight-membered rings parallel to *c*, formed by the neighbouring tetrahedral chains. Hence, the K ions occupy the same sites in the K-form that the Na atoms occupy in dehydrated natrolite. In the dehydrated K-form at 300 °C, the shift of K atoms is slight. The parameters *a* and *b* decrease by 11.1 and 7.6% due to dehydration (Table 5). As for natrolite, this decrease is considered to be caused by the rotation of the tetrahedral chain. The above-mentioned kinetic analysis shows that the dehydration of the K-form follows first-order kinetics. In the thermal decomposition of small solid particles, if the reaction rate is rapid, the decomposition proceeds particle by particle. Therefore, the reaction rate is proportional to the number of unreacted particles and the reaction follows first-order kinetics. In the K-form, since the shift of K ions due to dehydration is only small, it is suggested that the rate of propagation of the rotation of chains around *c* is so rapid that the dehydration is instantly completed in each particle. The dehydration then proceeds particle by particle. This is presumably why the dehydration of the K-form obeys first-order kinetics.

Summarizing the data obtained so far, the dehydration mechanism of natrolite and its K-form are interpreted as follows. The dehydration reaction occurs predominantly in the direction parallel to *c*. In natrolite, after the completion of dehydration, the propagation of the rotation of the chains of (Si, Al) tetrahedra and the contraction of the lattice occur simultaneously with the migration of Na ions, followed by the formation of the dehydrated phase. In the K-form, the propagation of the rotation of the chains occurs simultaneously with the progress of dehydration, and the dehydrated phase is formed at almost the same time that the dehydration is completed.

## ACKNOWLEDGEMENTS

The authors thank Drs. A. Kato and S. Matsubara, National Science Museum, for providing the natrolite sample. This study was partly supported by the Grant in Aid for the Scientific Research of the Ministry of Education, Japan (C-01550499).

## REFERENCES

1 W.O. Milligan and H.B. Weiser, J. Phys. Chem., 42 (1937) 1029.
2 M. Koizumi, Mineral. J., 1 (1953) 36.
3 C.J. Peng, Am. Mineral., 40 (1955) 834.
4 N. Imai, R. Otsuka and N. Yoshimura, Mem. School Sci. Eng., Waseda University, 28 (1964) 1.
5 R. Otsuka, H. Hayashi and N. Imai, Mem. School Sci. Eng., Waseda University, 34 (1970) 107.
6 L.P. van Reeuwijk, Meded. Landbouwhogesch. Wageningen, 74-9 (1974) 1.
7 W.M. Meier, Z. Krist., 113 (1960) 430.
8 J.H. Fang, Am. Mineral., 48 (1963) 414.

9 D.R. Peacor, Am. Mineral., 58 (1973) 676.
10 A. Alberti and G. Vezzalini, N. Jb. Miner. Mh., Jg. 1983 (1983) 135.
11 G. Gottardi and E. Galli, Natural Zeolites, Springer-Verlag, Berlin, 1985, p. 36.
12 S. Tanabe, Ph.D. Thesis, Waseda University, 1980.
13 A. Yamazaki and R. Otsuka, Thermochim. Acta, 109 (1986) 237.
14 A. Yamazaki, K. Kamioka, H. Matsumoto and R. Otsuka, Mem. School Sci. Eng., Waseda University, 118 (1987) 40.
15 A. Yamazaki, H. Matsumoto and R. Otsuka, Nendo Kagaku (J. Clay Sci. Soc. Jpn.), 28 (1988) 143.
16 T. Ozawa, Bull. Chem. Soc. Jpn., 38 (1965) 1881.
17 T. Ozawa, J. Therm. Anal., 9 (1975) 369.
18 C.D. Doyle, J. Appl. Polym. Sci., 5 (1961) 285.
19 J.D. Hancock and J.H. Sharp, J. Am. Ceram. Soc., 55 (1972) 74.